

# An Evaluation of Methods for Characterizing the Air / Water Interface for Parabolic Equation Transmission Loss Modeling

J. Paquin Fabre, Guy Norton, Robert Zingarelli, and Richard Keiffer

Naval Research Laboratory

Code 7180

Stennis Space Center, MS 39529 USA

**Abstract-** Proper characterization of underwater acoustic transmission loss (TL) relies on proper treatment of the air/water and water/sediment interfaces. This paper will focus on how the air/water interface is treated in parabolic equation (PE) models such as the range dependent acoustic model (RAM) [Collins, M. D., "Applications and time-domain solution of higher-order parabolic equations in underwater acoustics," *J. Acoust. Soc. Am.*, 86 (3), 1097-1102, 1989] and the finite element parabolic equation (FEPE) model [Collins, M.D., "A higher-order parabolic equation for wave propagation in an ocean overlying an elastic bottom", *J. Acoust. Soc. Am.* 86, 1459-1464, 1989]. Two surface loss methods have been implemented in RAM, a surface loss versus angle (LVA) and a conformal mapping (CM) method. Additionally, the CM method has been implemented in FEPE. These two methods are discussed and compared for realistic test cases and a third option, which has accuracy consistent with the CM but speed more aligned with the LVA approach is discussed.

## I. INTRODUCTION

In the operational modeling community, it is widely appreciated that acoustic propagation in the ocean can be strongly influenced by the presence of a surface duct (or half-channel) created between a near surface (local) maximum in the depth dependence of the sound speed and the pressure-release boundary at the air/sea interface. It is also recognized that, when present, the thickness of this energy trapping duct relative to the acoustic wavelength, the strength of the duct as characterized by the magnitude of the upward refracting gradient, and whether the source or receiver are located within or outside of the duct, are all important factors that influence the acoustic propagation [1].

It is because of the importance of this feature of the ocean-acoustic environment that the sonic layer depth (SLD), i.e., the distance from the air/sea interface to the local sound speed maximum, has become a widely used metric for sonar performance prediction. There has been significant research into the accurate approximation of the SLD (e.g. [2]) and SLD is frequently used as a metric for acoustic performance above cutoff frequency [3] in or near the layer. It is important to note, however, that the existence of a surface duct may be just one of several related ocean-acoustic phenomena. Wind is often the source of much of the turbulent mixing that can produce a surface duct but wind also creates a rough surface and breaking

waves inject air bubbles into the ocean. These commonly overlooked oceanographic features introduce scattering and frequency dependent refraction effects. We employ a high-fidelity finite element parabolic equation model with conformal mapping (FEPE-CM) that treats the air/sea roughness using a conformal mapping technique [4, 5] to demonstrate that these other ocean-acoustic phenomena should not be disregarded by the operational modeling community. Indeed, the results of the numerical modeling shown here argue that, as a general rule, SLD, which by itself "knows" nothing about the scattering from the air/sea interface or about the bubbles that may enhance it, should almost never be used by itself as a performance metric. That is, it is a better general policy to develop performance metrics that include the complications introduced by these other important (competing) ocean-acoustic phenomena.

It is generally accepted that current acoustic propagation models used for operational purposes have a limited ability to accurately estimate the effects of rough boundary scattering. The FEPE-CM model, while accurate, is too slow for operational purposes. Since it is believed that the FEPE-CM model addresses the important physics of the problem, the results of it can be used to help examine the accuracy of more approximate but commonly employed techniques for including the effects of scattering due to roughness into (operational) acoustic propagation models. Typical approaches employ a loss versus angle table that accounts for the *average* loss per interaction of sonic energy out of the (nominally) specularly reflected direction. This approach does not redistribute the acoustic energy scattered out of the specular direction and into any other directions. An examination of realistic test cases where a sonic layer was present using various surface loss modeling capabilities is presented. The results are compared and recommendations are made.

## II. OCEAN-ACOUSTIC PROCESSES

In the simulations that follow, the basic acoustic quantity of interest is transmission loss (TL). The aim of the simulations is to address the following questions: Given that a surface duct exists, how much does the inclusion of expected air/sea roughness and bubble-induced changes to the sound speed affect the TL? Are these changes significant enough to modify

how SLD is used as a performance predictor? Do the approximations and implementations employed by operational models to include roughness scattering adequately capture all of the important physics? In order to begin to answer these questions it is important to make clear the modeling assumptions and to discuss what are thought to be the main physical processes involved.

As mentioned previously, SLD is the depth below the air/sea interface at which a maximum in the sound speed occurs. It characterizes a surface duct, an ocean-acoustic phenomenon that frequently originates when turbulent (wind-driven) mixing creates an isothermal layer. In this well-mixed near-surface layer, the speed of sound increases with depth due to pressure effects, however, below the mixed layer the temperature in the ocean decreases and the sound speed (typically) becomes slower. This process results in a near-surface upward refracting sound speed profile. With the air/sea interface it forms a surface duct that can trap acoustic energy and, providing the duct persists over a large area, may result in very good long-range acoustic propagation. The surface duct and SLD are frequency-dependent concepts. Below a certain frequency the sound simply will not stay trapped in the duct.

The wind that is usually responsible for the turbulence that creates the mixed layer also roughens the sea surface and injects bubbles of air below the surface. These phenomena cause scattering and propagation effects that can strongly change the acoustic performance in and out of the surface duct. In some cases it is easy to envision how these other ocean-acoustic phenomena might conspire to diminish the energy trapping qualities of the surface duct. For example, scattering from a rough surface pumps energy out of the specular reflection direction and into all other propagation directions. Some of this redirected energy propagates at sufficiently steep angles to escape the surface duct. In other cases it is not at all clear which phenomena, if any, will dominate. For example, the energy trapping qualities of the surface duct are expected to improve with increasing frequency but the scattering also becomes increasing diffuse (more energy redirected out of specular) as the frequency increases. This is further complicated by the bubbles which can introduce strong frequency-dependent scattering and refraction effects.

Before leaving this section the concept of surface loss should be discussed. It is through this sonar equation based concept that most operational propagation models attempt to include scattering effects. Surface Loss (SL) is a derived quantity that is supposed to measure (in decibels) the average energy degradation experienced by an acoustic plane wave incident upon a rough interface [1]. It is parameterized by the angle of incidence, some measure of roughness statistics (typically the rms roughness, wind speed, significant wave height, etc.), and the acoustic wavelength. SL is derived from forward scatter measurements using modeled ray paths that know nothing about bubble-induced refraction effects. As such, SL estimates based on at-sea data unwittingly fold the net effects of several near-surface ocean-acoustic phenomena together into one quantity. It is a concept that is

most useful in the high frequency regime where ray theory applies and there is a clear correspondence between the ray trajectory at the interface and angle of incidence of the corresponding incident plane wave. Also, interactions with the interface can be unambiguously counted leading to the idea of a “loss per bounce”. SL characterizes the mean loss of acoustic energy out of the nominal reflection direction but does not address the redistribution of sonic energy into other forward or backward directions.

In wave theoretic solutions to the rough ocean waveguide problem SL loses its utility, or at least becomes more difficult to implement, precisely because those solution approaches are not typically amenable to a counting of discrete interactions with the interface, nor can the acoustic field incident upon or scattered from the rough interface be readily determined or (efficiently) decomposed into plane waves, nor can the far-field assumptions inherent in the concept of a “loss per bounce” scattering kernel be justified. These conceptual and implementation difficulties have not entirely excluded the application of the SL (“loss per bounce”) paradigm from wave theoretic acoustic propagation modeling, the fit is just a bit more of an approximation of convenience. For example, in marching and normal mode solutions the ray based concept of a cycle distance is borrowed to prevent the over-counting of loss due to scattering.

### III. SURFACE LOSS MODELING

Two phenomena should be considered when modeling the ocean surface, first the roughness of the surface and second the changes in the water column properties (particularly sound velocity) due to the bubbles. Next we will discuss the Loss versus Angle (LVA) method followed by the conformal mapping (CM) method with an algorithm to include the effect of bubbles on the sound speed.

#### A. Loss versus Angle Surface Loss

A way of including rough-surface effects on long-range TL in a gridded marching field propagation model such as RAM is described by Moore-Head et al. [6]. In that work, the vertical acoustic field in a thin near-surface layer is separated from the underlying field with a windowing function that smoothly tapers to zero at the bottom of the layer. In practice, the top half of the layer receives a weight of unity, while the bottom half of the layer is rolled off as a cosine function that crosses zero at the bottom of the layer. This portion of the field is then Fourier analyzed to decompose it into its angular components. It is then multiplied by a surface loss table [7] and a geometric ray cycle distance factor, and subsequently inverse Fourier analyzed back to depth space. This result is then spliced back onto the field values below the surface loss layer, and returned to the propagation model for the next range step.

While there is no true surface scattering in this algorithm, it can provide a useable approximation of the net effects for long range propagation. In order to enhance stability and reliability, several standard numerical techniques have been added in this current implementation. Chief of these is a linear windowing

function to damp and remove spurious high angle ( $>80^\circ$ ) rays that are not supported by the underlying propagation model, as well as a total energy check on the ingoing and outgoing field. The latter of these is particularly helpful when there is negligible loss from a nearly calm surface, and numerical noise boosts the outgoing field to slightly higher values than the incoming field. In such cases, the attenuated field is discarded and the original field is returned unmodified.

As straightforward as this algorithm seems, there are several details that can become problematic, given the wide variety of oceanographic environments encountered. Foremost of these is the choice of loss layer thickness. For the bulk of underwater environments, considering four acoustic wavelengths gives a reasonable balance between angular resolution requirements and the necessity of keeping this layer in some sense 'thin' and localized near the sea surface. Note also that the LVA algorithm assumes straight ray paths. A thinner loss layer will result in less refraction, causing inaccuracies in the angle of the rays as they reach the surface.

Refraction effects are a particular problem for this algorithm in environments with strong surface ducts. If the bottom of the loss layer coincides with the turning depth of most of the acoustic energy, any minor numerical problems can quickly accumulate. Extensive testing has shown that if ducting seems probable [1], it is best to place the layer bottom at twice the turning depth and adjust the cycle distance for ducted rays [8] accordingly.

### B. Conformal Mapping

Another approach to characterizing the surface in the TL model is the conformal mapping (CM) method. Here a summary of the implementation and validation of the CM technique in the FEPE model (FEPE-CM) is presented. For more details the reader is referred to Refs. 4, 5, 9, 10. The discrete rough surface is assumed to be a piecewise linear surface. The range step of the marching algorithm is chosen to be the grid spacing over which the rough surface is defined, hence at each range step only one segment of the piecewise linear surface is involved. That segment can be thought of as being the upper boundary of a trapezoidal 2-D section of the waveguide. By neglecting the bottom topography the geometry can be simplified even further, mapping one semi-infinite trapezoidal strip onto a rectangular strip. This is a valid approximation because the effect of the surface roughness on depth through the mapping extends only a few meters from the surface. The local angle of inclination of the surface segment is represented through the non-dimensional parameter  $\nu$  (fraction of  $\pi$ ). For all practical applications, the effect of the surface roughness on depth through the conformal mapping is extinguished well before reaching the bottom. Only one segment of the surface is mapped at a time, using a different conformal mapping for each range step. The marching algorithm is implemented in a transformed or *pseudospace*. The field is advanced one range step in pseudospace and then transformed back to physical space. The solution to the original rough surface problem has been advanced one range step in physical space and the previous pseudospace is discarded.

Dozier [9] has shown that each local conformal mapping transforms the elliptic wave equation into another elliptic equation of the same form in the transform space. That is, the wave equation in the physical space  $(r, z)$  defined by the trapezoidal strip, is transformed into a flat surface rectangular strip in pseudospace  $(\tilde{r}, \tilde{z})$ . The wave equation in pseudospace has the same form as in physical space, with a modified sound speed profile given by

$$\tilde{c}(\tilde{r}, \tilde{z}) = \frac{c[r(\tilde{r}, \tilde{z}), z(\tilde{r}, \tilde{z})]}{|f'(\tilde{z})|}, \quad (1)$$

where  $f'(\tilde{z})$  is the magnification factor of the mapping. This factor is either larger or smaller than unity but, in all cases, tends rapidly toward unity as depth increases.

The net result of the conformal mapping technique is then to convert a rough surface scattering problem into a succession of locally flat surface problems, each one with its own modified sound velocity profile. Even if the original sound velocity profile (i.e. in physical space) is isovelocity, in pseudospace where the "ocean surface" is flat, it becomes depth and range dependent (due to the magnification factor). At each range step there is a unique velocity profile in physical space and two velocity profiles in pseudospace, one associated with the left side and the other with the right side of the surface segment. Each profile leads to a different unevenly spaced mesh in physical space. FEPE is marched over the range step in pseudospace making use of the average profile, whereupon the result is transformed back to physical space.

The FEPE-CM technique for handling surface roughness has been thoroughly validated by Norton *et al.* [5] by comparison with a full wave scattering model for the case of periodic surfaces, as well as for single realizations of randomly rough surfaces having a power spectrum characteristic of a sea surface.

### C. Plumes Bubble Modeling

In underwater acoustics, the compact assemblages of bubbles introduced by breaking waves are usually referred to as clouds or plumes. Thorpe [11], who was among the first to describe these compact assemblages, used the term "clouds" and made a distinction between two types of clouds depending on the buoyancy flux characterizing the air-sea interchange. Crawford and Farmer [12] refer to both plumes and clouds without distinction and describe clouds or plumes superimposed on a persistent "near-surface bubble layer." They also stated that "the plumes appear to be roughly v-shaped, decreasing in width with depth." Monahan [13,14] discretized the time evolution of a bubble plume into three stages  $\alpha$ ,  $\beta$ ,  $\gamma$ , and associated two of them with two stages of whitecaps. Novarini *et al.* [15] utilized Monahan's description and developed a model for the range and depth dependence of the bubbly environment. This model, which generates a possible realization of the bubbly environment from inputs of wind-speed, duration, and fetch then calculates the frequency-

dependent change in the sound speed and attenuation induced by the presence of the bubble plumes.

#### IV. RESULTS

The LVA, FEPE-CM and FEPE-CM with plumes techniques were all applied to two realistic test cases for a fairly deep area where a sonic layer exists and would trap above approximately 400 Hz. The sonic layer is  $\sim 350$  m in depth at the source and the source is placed in the layer at 50 m depth. The water depth is approximately 2000 m and the acoustic models were run to a range of 50 km. Two frequencies are examined, 400 Hz, near cutoff and 800 Hz, well above cutoff.

For the purposes of a baseline, the first TL prediction studied is the flat surface using the RAM model. Figure 1 shows the results for 400 Hz and Figure 2 for 800 Hz. It can be seen that the duct is trapping a significant amount of energy at 800 Hz and less at 400 Hz, indicating that propagation in the duct is favorable at 800 Hz. However, the wind speed in this case is approximately 17 m/s, which is significant, therefore, the next prediction (Figure 3) shows the RAM model run with the appropriate wind speed using the LVA algorithm as described in Section III. A. As expected, differences are apparent between this and the flat case, the trapping is still evident, but doesn't travel as far in the duct, and less energy is transmitted below the duct down-range.

The more accurate FEPE-CM method was run for the 17 m/s wind speed case, with and without bubbles. Figure 4 shows the top 500 m of this environment with the CM rough surface for 17 m/s, Figure 5 includes the bubble field only and Figure 6 shows the CM rough surface with the bubbles. The CM rough surface with bubbles (Figure 5) contains the most physics, is the most realistic case, and is considered to be the model benchmark. The rough surface introduces many interference patterns (Figure 4) and the bubbles "cushion" this effect while attenuating the energy (Figure 6). The loss is significantly affected and impacts the energy trapped in the duct, as can be seen by comparing Figure 2 to Figure 6. Comparing Figure 6 to Figure 3, it can be seen that the loss is significantly under predicted using the LVA approach.

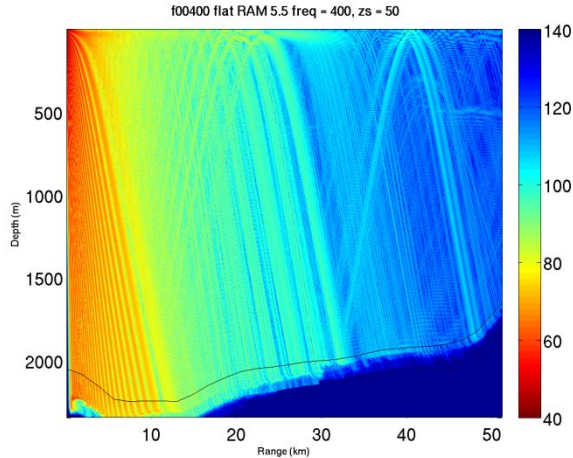


Figure 1. Flat surface RAM prediction for 400 Hz.

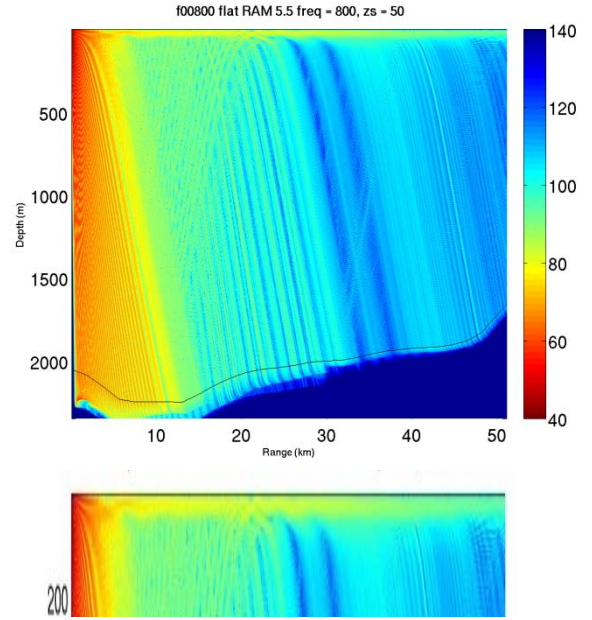


Figure 2. Flat surface RAM prediction for 800 Hz, full waveguide (top) shallowest 200m (bottom).

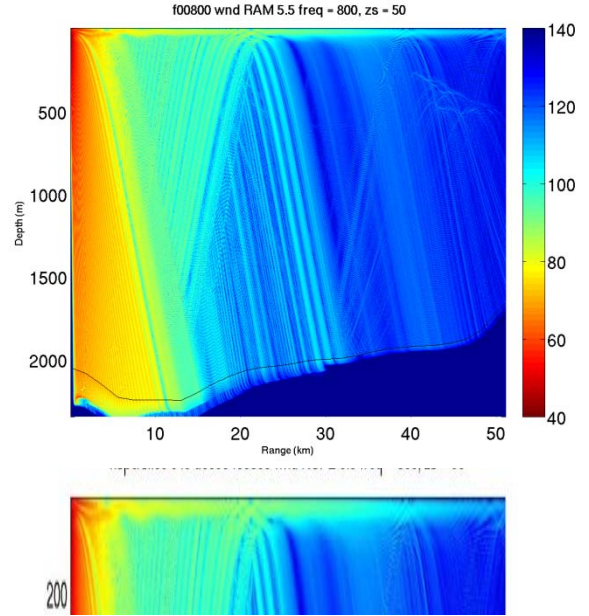


Figure 3. RAM with LVA for 17 m/s wind speed at 800 Hz, full waveguide (top), shallowest 200m (bottom).

In order to more closely examine the differences, all modeling configurations are plotted in Figure 7 for a 20 m receiver in the center of the duct and in Figure 8 for a 200 m receiver below the duct. The LVA (black line) differs by more than 15 dB from the benchmark (light orange line; rough surface and bubbles) at the maximum range (50 km). Below the duct, the lines seem to compare more favorably at maximum range, but differ by up to  $\sim 10$  dB at mid-range due to the difference in the energy between convergent zones that is evident in Figure 3 and Figure 6 between 20 and 40 km.



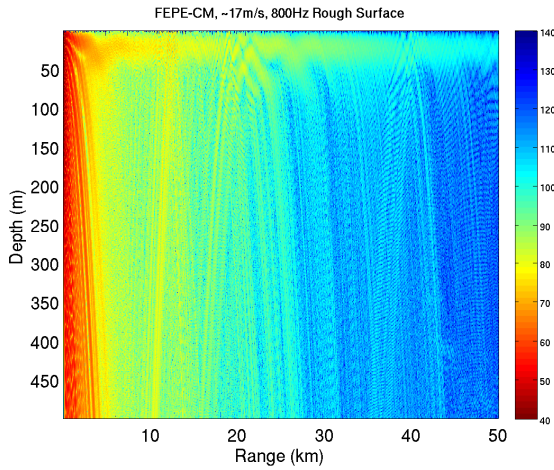


Figure 4. Predicted TL using FEPE-CM with 17 m/s rough surface for 800 Hz.

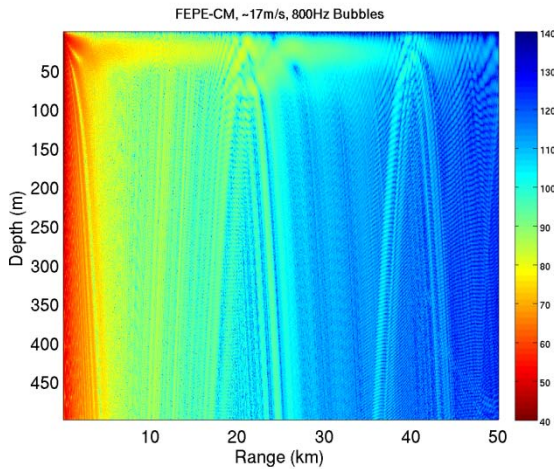


Figure 5. Predicted TL using FEPE-CM with 17 m/s bubbles field for 800 Hz.

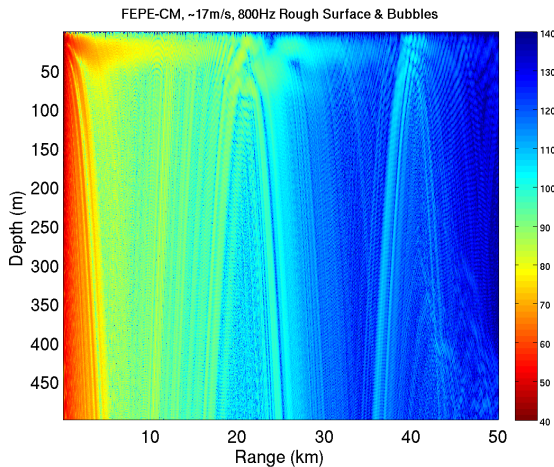


Figure 6. Predicted TL using FEPE-CM with 17 m/s rough surface and bubble field for 800 Hz.

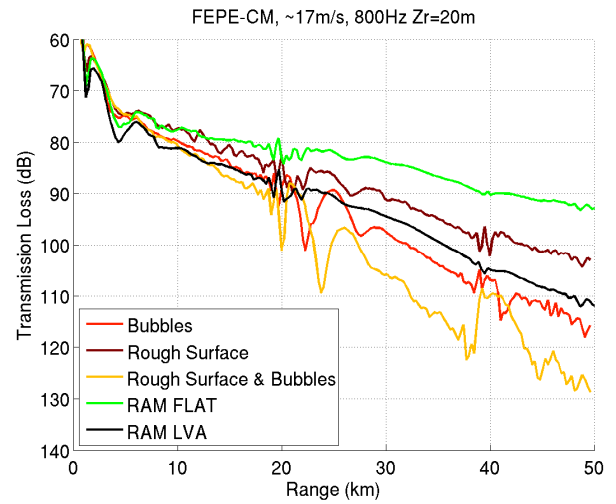


Figure 7. TL versus range for 17m/s, 800 Hz case for a 20m receiver in the duct for the five modeling configurations discussed.

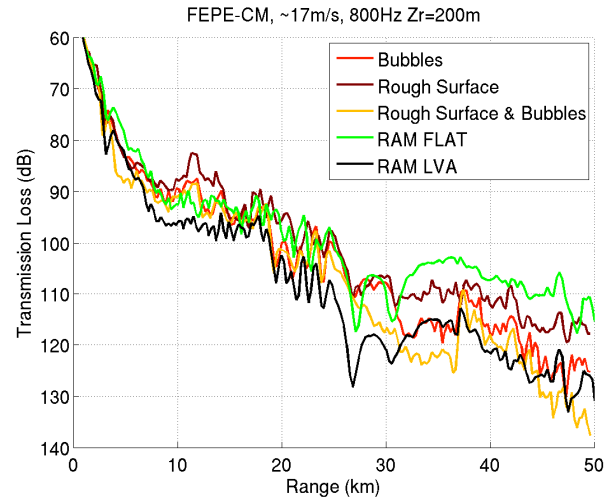


Figure 8. TL versus range for 17m/s, 800 Hz case for a 200m below the duct for the five modeling configurations discussed.

A second example was chosen with a lower wind speed to represent a more operationally feasible environment. The acoustic models were applied to this test case for a slightly shallower area where a sonic layer exists and would trap approximately 300 - 400 Hz and above. The sonic layer is approximately 250 m in depth at the source and the source is again placed in the layer at 50 m. Two frequencies were again examined, 400 Hz, near cutoff and 800 Hz, well above cutoff and the 800 Hz results to 50 km are shown here.

Figure 9 shows the top 500 m of the RAM flat surface case at 800 Hz, where again, the trapping is evident. As before, the RAM LVA was run and as seen in Figure 10, the energy does not travel as far in the duct due to the lossy surface.

Next the rough surface and bubble modeling was included. Figure 11 shows FEPE-CM transmission loss with the rough surface and Figure 12 includes the bubbles. Figure 13 shows the sound speed near the surface as modified by the plumes bubble model. The beta plumes are smaller and are characterized by sound speeds as low as 700 m/s and the

gamma plumes cover more of the surface layer and are characterized by sound speeds close to that of the water near the surface,  $\sim 1540$  m/s. Figure 14 shows transmission loss for both rough surface and bubbles for the 8 m/s case. In comparing Figure 14 to Figure 10 differences in the energy in the duct are evident and there is more energy below the duct as a result of the high angle scattering off the rough surface.

Depth slices were again examined in and below the layer. In the layer, shown in Figure 15, the LVA (black) compares favorably with the benchmark bubbles and rough surface case (light orange). However, below the layer, shown in Figure 16, the LVA over-predicts the loss by up to 15 dB due to the high angle scattering imposed by the rough surface. The LVA modeling is more likely to be relied upon in these lower wind speed scenarios, so the over-prediction of the loss could lead to incorrect decisions.

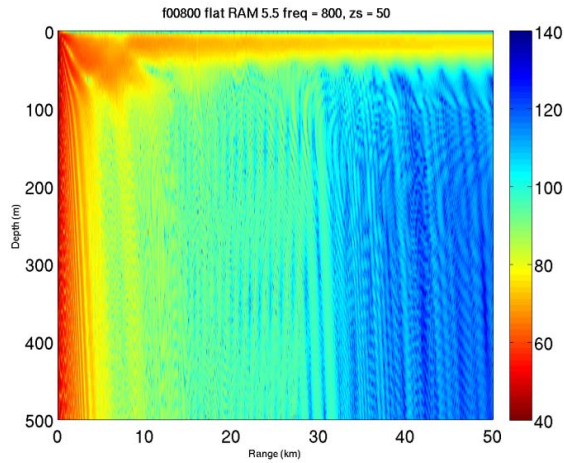


Figure 9. RAM flat surface for lower wind speed scenario.

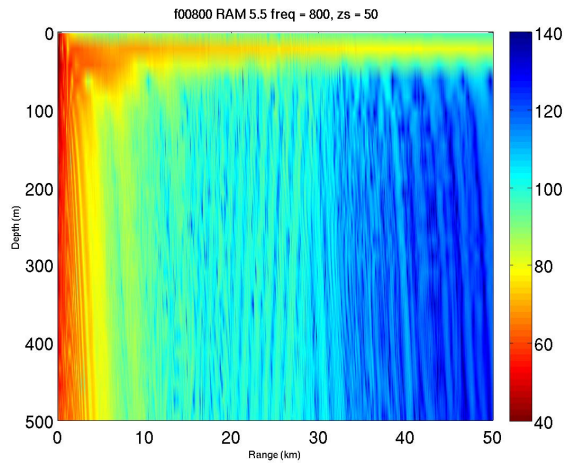


Figure 10. RAM LVA for 8 m/s wind speed case.

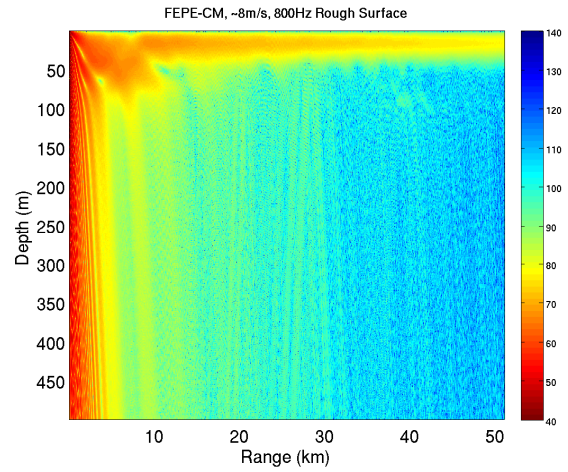


Figure 11. FEPE-CM prediction with rough surface 8 m/s.

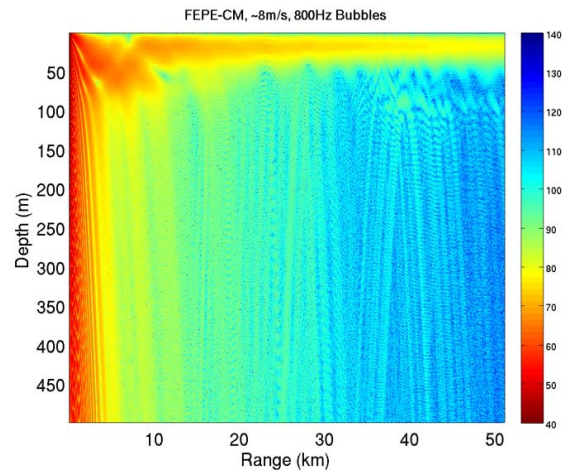


Figure 12. FEPE-CM prediction with bubbles for 8 m/s.

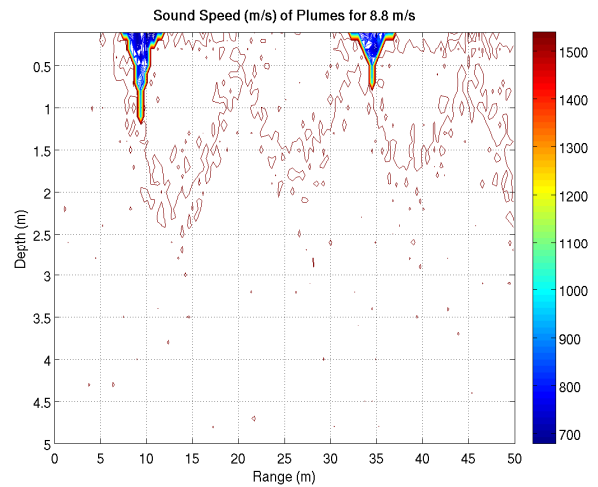


Figure 13. Sound speed in the top 5m of the waveguide to 50m in range, as modified by the plumes model for an 8 m/s wind speed.



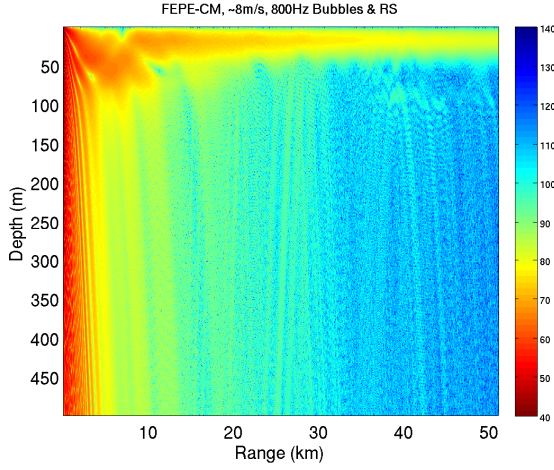


Figure 14. FEPE-CM prediction with bubbles and rough surface for 8 m/s.

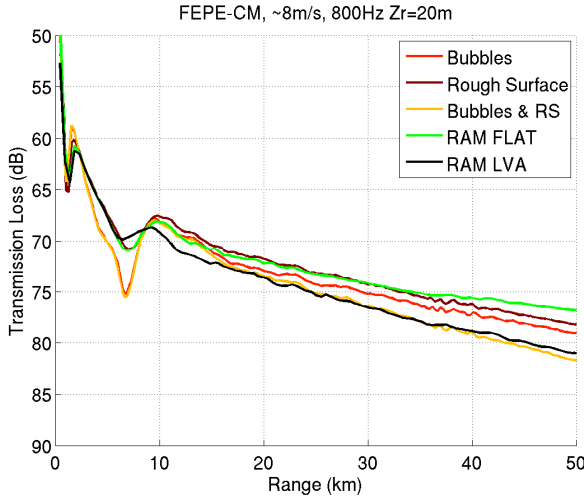


Figure 15. TL versus range for a 20m receiver in the duct for the five 8 m/s wind speed modeling scenarios.

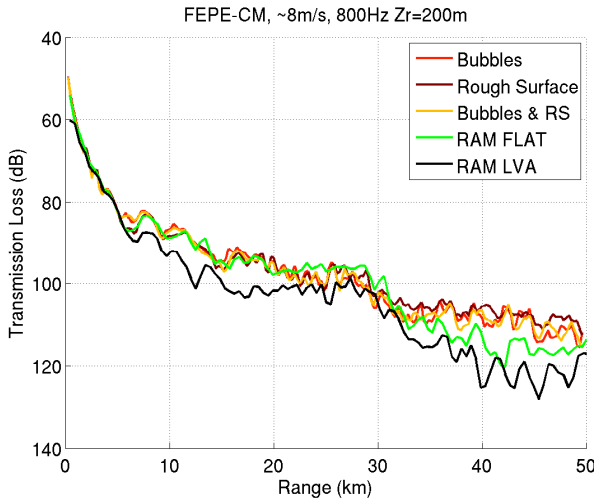


Figure 16. TL versus range for a 200m receiver below the duct for the five 8 m/s wind speed modeling scenarios.

## V. CONCLUSIONS

Realistic test cases of acoustic propagation in a surface duct have been examined using two surface loss algorithms: a LVA and a benchmark that includes rough surface and bubble characterization. The faster LVA algorithm does not consistently predict the loss in a ducted environment for significant wind speeds. The rough surface capability with bubbles gives accurate benchmark results, but is too computationally intensive for everyday use; it can however be used for fine tuning the existing surface loss algorithm accuracy. Subtle improvements, such as possible modifications in angle interpolation schemes or ray cycle distance normalization factors, that would not significantly affect the previous single surface bounce testing, should be evident in comparisons with these accurate long-range results.

Three ways of incorporating the refractive effects of surface bubble layers into the RAM model for faster, more accurate predictions are possible. First, directly modifying the sound speed profile, next mapping the bubble effects into a change in propagation angle within the surface loss routine and finally, mapping the bubble effects into a change in the surface loss table. Of these three possibilities the latter seems the most likely to give satisfactory results, however it will require the most analytic development. We anticipate that comparisons with benchmark answers will decide the final form of the integration.

## ACKNOWLEDGMENT

Thank you to the Naval Research Laboratory Base Program and the Office of Naval Research for encouraging and funding this effort.

## REFERENCES

- [1] R. J. Urick, Principles of Underwater Sound, New York: McGraw-Hill, pp. 149–151, 1983.
- [2] Robert W. Helber, Charlie N. Barron, Michael R. Carnes, and Robert A. Zingarelli, "Evaluating the sonic layer depth relative to the mixed layer depth," *J. of Geophys. Resch*, vol. 113. C07033, 2008.
- [3] [http://en.wikipedia.org/wiki/SOFAR\\_channel](http://en.wikipedia.org/wiki/SOFAR_channel)
- [4] M. D. Collins, "Applications and time-domain solution of higher-order parabolic equations in underwater acoustics," *J. Acoust. Soc. Am.*, vol. 86(3), pp. 1097-1102, 1989.
- [5] G. V. Norton, J. C. Novarini, and R. C. Keiffer, "Coupling scattering from the sea surface to a one-way marching propagation model via conformal mapping: Validation," *J. Acoust. Soc. Am.* **97**, 2173-2180, 1995.
- [6] M. E. Moore-Head, W. Jobst, and E. S. Holmes, "Parabolic-equation modeling with angle-dependent surface loss", *J. Acoust. Soc. Am.* **86**, 247-251, 1989.
- [7] C.S. Clay, "Fluctuations of sound reflected from the sea surface," *J. Acoust. Soc. Am.*, **32**, pp. 1547-1551, 1960.
- [8] C.S. Clay and H. Medwin, Acoustical Oceanography, New York: John Wiley & Sons, pg. 87, 1977.
- [9] L. B. Dozier, "PERUSE: A numerical treatment of rough surface scattering for the parabolic wave equation," *J. Acoust. Soc. Am.* **75**, 1415-14432, 1984.
- [10] G. V. Norton and Novarini, J. C., "The effect of sea-surface roughness on shallow water waveguide propagation: A coherent approach," *J. Acoust. Soc. Am.* **99**, 2013-2021, 1996.
- [11] Thorpe, S. A., "On the clouds of bubbles formed by breaking waves in deep water and their role in the air-sea gas transfer," *Philos. Trans. R. Soc. London, Ser. A* **304**, 155-210, 1982.

- [12] Crawford, G. B., and Farmer, D. M., "On the spatial distribution of ocean bubbles," J. Geophys. Res. **92**, c8, 8231-8243, 1987.
- [13] Monahan, E. C., "Whitecap coverage as a fully monitor able indication of the rate of bubble injection into the oceanic mixed layer," in *Sea Surface Sound*, edited by B. R. Kerman (Academic, New York), pp. 85-96, 1988.
- [14] Monahan, E. C., "Occurrence and evolution of acoustically revelant sub-surface bubble plumes and their associated, remote monitorable, surface whitecaps," in *Natural Physical Sources of Underwater Sound*, edited by B. V. R. Kerman (Kulwer Academic, Dordrecht), pp. 503-517, 1993.
- [15] Novarini, J. C., Keiffer, R. S. and Norton, G. V., "A model for variations in the range and depth dependence of the sound speed and attenuation induced by bubble clouds under wind-driven sea surfaces," IEEE J. Ocean. Eng. **23**, 423-438, 1998.